

Designing False Data Injection Attacks Penetrating AC-based Bad Data Detection System and FDI Dataset Generation

Nam N. Tran | Hemanshu R. Pota | Quang N. Tran | Xuefei Yin | Jiankun Hu*

School of Engineering and Information Technology, University of New South Wales Canberra at ADFA, Australian Capital Territory 2620, Australia

Correspondence

*Jiankun Hu, School of Engineering and Information Technology, University of New South Wales Canberra at ADFA, Australian Capital Territory 2620, Australia. Email: jhu@adfa.edu.au

Summary

The evolution of the traditional power system towards the modern smart grid has posed many new cybersecurity challenges to this critical infrastructure. One of the most dangerous cybersecurity threats is the False Data Injection (FDI) attack, especially when it is capable of completely bypassing the widely deployed Bad Data Detector of State Estimation and interrupting the normal operation of the power system. Most of the simulated FDI attacks are designed using simplified linearized DC model while most industry standard State Estimation systems are based on the nonlinear AC model. In this paper, a comprehensive FDI attack scheme is presented based on the nonlinear AC model. A case study of the nine-bus Western System Coordinated Council (WSCC)'s power system is provided, using an industry standard package to assess the outcomes of the proposed design scheme. A public FDI dataset is generated as a test set for the community to develop and evaluate new detection algorithms, which are lacking in the field. The FDI's stealthy quality of the dataset is assessed and proven through a preliminary analysis based on both physical power law and statistical analysis.

KEYWORDS:

Bad Data Detector, cyber-physical system, cyberthreat, False Data Injection Attack, power system, smart grid, State Estimation

1 | INTRODUCTION

The prominence of deploying information and communication technology in the traditional power system integrated with Distributed Energy Resources (DERs) such as solar, wind, energy storage, etc., has gradually revolutionized this infrastructure into a much more advanced cyber-physical system, called smart grid. Such transformation offers various benefits to the task of system monitoring and management which is undertaken by the Energy Management Systems (EMSs). It also introduces many new kinds of cyber-threats to the system. The core part of an EMS is the State Estimation (SE), which is assigned to do multiple tasks, including collecting and processing measurements, removing inadequate data, and solving an optimization problem to yield a set of state variables that closely reflect the status of the system. As the whole process involves data transmission over communication networks, problem of measurement data being compromised are emerging and getting more and more attention in the field.

Among all kinds of threats, a new type called False Data Injection (FDI) attack is considered extremely dangerous as it is completely stealthy under examination by the State Estimation, as shown in Liu et al.¹ and Hug et al.². FDI attacks aim directly at the set of measurements by injecting manipulated data, thus driving the system's behavior in a malevolent way. From the view point of the adversaries, this man-in-the-middle type of attack is an effective method to mislead the operators at the control center. For instance, an FDI attack might lead the SE to indicate some surges of power flow on lines, which could make the operators to think about the malfunctioning of the automatic relay protection system. As a result, the operators might establish an emergency protective mechanism to trip down the suspected lines, which might possibly bring out power outages.

Since the discontinuity of power supply is a severe incident due to its consequences, it is apparent that FD I attack can inflict damage to the physical system as well. In another situation, an FD I attack might help hackers to take advantage by changing power consumption at some specific nodes, which will result in significant errors in load forecasting and generation planning.

Most of existing research works in this field are based on the simplified DC model, e.g., Liu et al.¹, Bobba et al.³, and Anwar et al.⁴. However, it is important for researchers and industrial professionals to understand the FD I's stealthy capability under the AC-based practical setting model, which has been widely deployed in the industry. In this paper, a comprehensive FD I attack design scheme is presented to examine its effectiveness using fully nonlinear AC power flow model. Thus, it is much more challenging than most of the previous works which were purely based on simplified linearized DC-based models. The proposed FD I attack scheme has been tested on a case study to assess its capability to penetrate a commercial-level AC based SE package, PowerFactory 2017 SP4 from DigSILENT⁵. As demonstrated by the experimental results, our proposed method of FD I attack has successfully exploited a critical vulnerability in the state-of-the-art Bad Data Detector (BDD) and plausibility checking. As both the existing detection methods with electrical (for plausibility checking) and stochastic (for bad data removing) basis have failed to accomplish their missions, new FD I attack detection mechanisms are needed. Unfortunately there exist no realistic AC-based FD I attack dataset publicly available, which has greatly hindered the relevant technology development in terms of designing new FD I attack detection mechanisms and their evaluation. In order to provide a practical tool to evaluate FD I detecting techniques, a cyber-physical dataset is constructed and released publicly. Unlike the case of pure cyberspace environment which has several datasets for testing design theories (for instance KDD⁶, DARPA⁷, ADFA-LD^{8,9}, NGIDSDS¹⁰, etc.), to the best of our knowledge, our FD I dataset is the first ever AC-based FD I dataset. It has been created with highly realistic settings as a result of a combination of the use of an industry-standard commercial-level package (PowerFactory) as the test platform, a trusted source of input data (Australian Energy Market Operator), and a sophisticated attack design process presented in this paper. We also provide some preliminary analyses in order to demonstrate the cause for the failure of BDD equipped with this SE package.

The primary contributions from this paper can be summarized as follows:

1. Providing an evaluation, using a commercial SE package, of the performance of DC-based FD I attack model against an AC-based system. Note that most of the FD I detection schemes are based on DC-based FD I attack model and have been evaluated in a simplified simulation setting. It is important and also interesting to observe the behavior of the system in commercial-scale settings that are used in real systems.
2. Proposing a systematic AC-based FD I attack design scheme. An experimental case study is provided, which shows the success of perfectly bypassing a BDD in commercial-level SE package.
3. Generating the first cyber-physical FD I attack dataset for public research purpose.
4. Providing preliminary analyses to explain the failure of the state-of-the-art BDD against our proposed attack scheme.

The organization of this paper includes six sections with the current section being the introduction of the research problem. Section 2 reviews various related work and also provides an assessment of some popular DC-based attack schemes against AC-based SE. Section 3 presents a comprehensive attack design scheme based on the AC model of power flows. Based on the proposed design scheme, a large-scale cyber-physical FD I attack dataset is generated which is described in Section 4. Section 5 provides preliminary analysis from both electrical and stochastic perspectives in order to highlight the stealth quality of the generated FD I dataset. Conclusion and some future researches are given in Section 6.

2 | PREVIOUS WORK

Due to the advent of the pioneering work by Liu et al.¹, there have been myriads of publications on the FD I attack against SE in power system. Liu et al.¹ comprehensively categorized almost every type of FD I attack. One limitation of this work is that the linearized DC-based power flow model is deployed to test the attacks. Despite the authors' claim to expand their future research into the field of nonlinear AC-based model, most of, if not all, following works still applied the DC-based model. According to the review in Liang et al.¹¹, it pointed out that in the field of FD I attack research including types, impacts and defense strategies, DC-based publications still dominate the literature.

Sharing the same foundation of DC power flow model, Yang et al.¹² proposed an optimized way to attack with minimum effort, and Rahman et al.¹³ confirmed that an attack without complete knowledge about the system is possible. Similar to the work of Yu et al.¹⁴ where a proposed attack scheme was based on the Principal Component Analysis to aim at creating a blind FD I attack, Esmaeilifalak et al.¹⁵ assumed loads are invariant and then formed an attack based on the Independent Component Analysis for stealthy purpose. Liu et al.¹⁶ introduced a strategy to determine optimal attack region given the limited network information. Meanwhile, Adnan et al.⁴ tried to construct an attack by building up low-rank original measurement matrix from observed measurement matrix. Kim et al.¹⁷ introduced a variant of FD I attack named Data Framing which is unable to completely bypass the BDD but is sophisticated enough to deceive the Bad Data Identification (BDI), thus mislead the SE to produce incorrect system's states. During this period, several research groups also published various defense strategies against FD I attack, including heuristic¹⁸, protecting right from

the measurement³, Sparse Optimization¹⁹, using sequential detector²⁰ or adaptive CUSUM test²¹ and even a graphical method²². All of these defense schemes are planned with great details and some even mention the financial consequences²³. These results have greatly contributed to the advancement in this field. However, whether or not such works are applicable for the AC model based realistic systems is an open question.

For its simplicity, there is no doubt that the DC-based model is a good starting point for FD research. With the development of computing technology, the problem of computational cost or convergence issue can no longer hinder the implementation of AC-based SE in the EMS. By removing several simplified assumptions, AC-based model can provide a better estimated set of results. This fact can be easily confirmed once we investigate the fundamental power flow equations and measurement model for each type:

- DC power flow equation: $P_{ij} = \frac{\theta_i - \theta_j}{X_{ij}}$.
- DC measurement model: $z = \mathbf{H}x + \epsilon$.
- AC power flow equation: $P_{ij} = f(V_i, V_j, g_{ij}, b_{ij}, \theta_i, \theta_j)$
- AC measurement model: $z = \mathbf{H}(x) + \epsilon$

The difference between these two models is quite significant as the AC model also takes into account the equation for reactive power flows. Consequently, it is highly possible that any designated technique for DC-based model will not work well with an AC-based SE. For illustration purpose, we conducted a test with the WSCC's 9-bus system following the primitive attack method against the SE package in PowerFactory 2017. As claimed by Adnan et al.²⁴, a random contaminated vector \mathbf{C} in conjunction with the system Jacobian matrix \mathbf{H} whose elements are partial derivatives of power flow equations, will be enough to produce an attack vector $\mathbf{a} = \mathbf{H}\mathbf{c}$ that could successfully bypass BDD in an SE. Assuming the \mathbf{H} matrix has already been acquired, we randomly generated 100 different vectors \mathbf{C} to create 100 sets of corrupted measurements accordingly. After feeding measurement values respectively into the PowerFactory's SE, we achieved two types of outcomes: 46 cases failed to converge while 54 cases converged successfully but none has been able to completely bypass the BDD as expected. Moreover, the existence of manipulated measurements also resulted in the false alarm of some other good measurements. From these experimental results, designing FD attack derived from DC power flow model is unlikely to possess its stealthy characteristic against an industry-standard AC-based SE. Such failures of DC-based design were also recognized in Huget al.², Manandhar et al.²⁵, Chaojin et al.²⁶, Liang et al.²⁷ and Rahm et al.²⁸ as various methods were proposed to produce corrupted AC power flow model measurement values. As these works did not state explicitly the examination environment to test their designs, the first target that has inspired our work is designing an attack to completely bypass the more realistic nonlinear AC model based BDD. In addition, it is equally important to generate the first FD dataset as a benchmarking tool for conducting research in evaluating their proposed FD detection solutions.

3 | DESIGN SCHEME AND EXPERIMENTAL RESULT OF AN FD ATTACK AGAINST AC STATE ESTIMATION IN POWER SYSTEM

3.1 | Design principle

Technically, the transmission system for SE research is particularly considered as a quasi-static model whose variables are constantly yet slowly changing. The task of system monitoring is conducted in a discrete manner by the means of gathering data about the system, then building up a snapshot that reflects the current state. This process is repeated after an interval, generally about 5 to 10 minutes. From an attacker's point of view, the process to generate an FD attack includes two main stages: (S1) Collecting data about the current state of the system (or a subsystem of interest); (S2) Designing the malicious measurement values and then injecting them into the data acquisition system. The second stage can be divided into five tasks, corresponding to: identifying Area of Attack, forming constraint equations, identifying changeable state variables, initializing adjustment and solving equations, and computing with the corrupted measurements. If the attackers already have enough information about the configuration of the system or subsystem, i.e. (S1) is done, it will take almost no time to design a completely stealthy attack (S2) with our proposed attack design scheme. In this paper, we will focus on the mission of systematically calculating the manipulated values of measurements (S2), whose sub-stages are shown in Fig. 1 in order to completely bypass the existing BDD⁵.

Since this work mainly concentrates on the design process of malicious values, several assumptions are made in this study. Firstly, attackers can collect the data relevant to one state of the system (or a subsystem of interest), including topology, status of the breakers and transformer taps, state variables (voltage magnitudes, voltage angles), power flow measurements (both active and reactive powers) on branches, and power injection measurements at nodes. Secondly, the attackers are able to not only retrieve data from the system but also overwrite the values sent by measurement devices to the control center. In addition, all the measurement devices are considered having the same accuracy and weight. Such a situation can arise when either the working computer or working account of the operator is compromised. Such assumptions have been used in most of FD based applications^{2,25,27}.

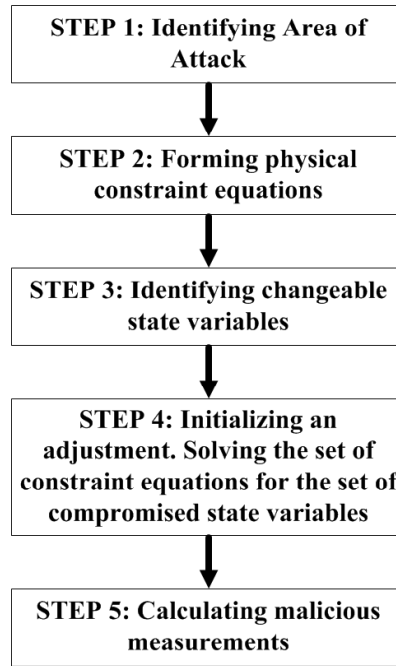


FIGURE 1 Details of Stage (2) in the FD I attack design scheme to generate an FD I attack – Design the malicious measurements.

3.1.1 | Attack Area

From the view point of state estimation, the state of being injected by an FD I attack is equivalent to a new steady state, which consists of both genuine as well as manipulated measurement values. In other words, FD I attack will replace a set of system's measurements by another set that contains either only manipulated measurement values or both unchanged and corrupted values. In fact, it is reasonable for the attacker to only aim at adjusting a set of values in a subsystem or a sub-grid rather than taking risk of probably being detected due to attacking on a wide area. The smaller the affected area is, the higher the chance that the attack is hidden. The affected or attack area here is defined as a region that consists of all branches whose power flows are altered. Thus, the boundary of this region is formed by a set of nodes that are intersections of at least one affected branch to one or several branches with no corrupted power flows.

The first and foremost task in identifying the area of attack is finding its boundary. According to Hug et al.², the condition for a stealthy FD I attack is partly satisfied if the area of attack has the boundary of all power-injection nodes. Unlike the traditional way to categorize buses in bad flow calculation, the FD I attack design process only separates bus type into two groups: (B_1) bus *with power injection* (either incoming or outgoing) and (B_2) bus *with no power injection*. The reason that the area of attack must be enclosed by only (B_1) buses is due to the fact that an FD I attack alters the measurement values at both ends of every branch within the range of attack. Since, at every (B_2) bus, the Kirchhoff's Current Law must be satisfied, this kind of bus will force at least one connected branch's power flows to be changed. Consequently, the existence of (B_2) bus will result in the expansion of area of attack. Such expansion will be continued till there is no bus on the boundary belonging to (B_2) type. For instance, consider two connected branches (a-b) and (a-c) with a common terminal a being of (B_2) type. Any change of power flow happens on (a-b) will result in at least another couple of changes on branch (a-c) since the algebraic sum of power flows at node a must be equal to zero. In order to make these changes to be reasonable, the terminal c of the latter branch must have power injection there. An illustrative example about this statement is provided in Hug et al.².

In this work, the process of identifying FD I attack area is conducted by using an *extended admittance matrix* Y_{bus} . The extended Y_{bus} for an n -bus system is a matrix that has size of $n \times (n + 1)$. Its formation is based on the horizontal concatenation of the traditional admittance matrix Y_{bus} with an additional column, which has the information about the type of the node. Elements of the additional column have values of either 0 or ± 1 , depending upon whether a bus is of no-injection or power injection type. The bus that has power injection is further distinguished by a sign in order to support the process of automatic design attack, with +1 denoting a bad and -1 denoting a bus with power going out. The Algorithm 1 presents the area of attack identification process.

Algorithm 1 Identifying Area of Attack

Input: Extended Y_{bus} , Central node i Output: Area of Attack Ω_A

```

1: <1> Look for  $i^{\text{th}}$  column of the extended  $Y_{bus}$ 
2: <2> Obtain  $\Omega_i = \{j | Y_{ji} \neq 0\}$ 
3: <3> Scanning process:
4: while  $j \in \Omega_i$  do
5:   if  $(Y_{j(n+1)} \neq 0)$  then
6:     if (Last of  $\Omega_i$ ) then
7:        $\rightarrow$  Jump to <4>
8:     else
9:        $j++$ 
10:    end if
11:  else
12:    Do <1> -<3> with new central node  $j$  (and its list  $\Omega_j$ )
13:  end if
14: end while
15: <4> Add up all  $\Omega_i + \Omega_j \dots$  to obtain the Area of Attack  $\Omega_A$ 

```

3.1.2 | Constraint Equations and Changeable State Variables

The next step in the attack design process is setting up the set of physical constraint equations by the use of Algorithm 2. Its solution is the essential resource for computing the manipulated measurements, which, in turn, will effectively bypass the BDD of AC-based SE. The number of the constraint equations depend on the configuration of the system or the subsystem, particularly, the number of no-injection nodes within the area of attack. The formation of the constraint equations originates from the Law of Conservation of Energy²⁹, which offers a smooth transition from a steady state of operation (the genuine one) to another steady state of operation (the corrupted one), thus, guaranteeing the stealthy characteristic of the attack. Since the state of being attacked by FD I technique is essentially a counterfeit steady state, it must satisfy the following two constraints:

- The sums of active and reactive power flows at any no-injection node must be equal to zero. Thus, for any no-injection Bus j , we have: $\sum_j P_{jk} = 0$ & $\sum_j Q_{jk} = 0$.
- All the changes in power injections (both active and reactive) at nodes as well as power losses (both active and reactive) on branches must add to zero. Therefore we have the constraint as: $\sum \Delta P_{INJ} + \sum \Delta P_{LOSS} = 0$ & $\sum \Delta Q_{INJ} + \sum \Delta Q_{LOSS} = 0$.

Algorithm 2 Forming physical constraint equations

Input: Extended Y_{bus} , Central node i , Area of Attack Ω_A Output: The set of constraint equations S

```

1: while  $(j \in \Omega_A)$  and  $(Y_{ij} \neq 0)$  do
2:   if  $(Y_{j(n+1)} = 0)$  then
3:     Write  $\sum_j P_{jk} = 0$ 
4:     Write  $\sum_j Q_{jk} = 0$ 
5:   else
6:     Write  $\sum_j \Delta P_{INJ} + \sum_{jk} \Delta P_{LOSS} = 0$ 
7:     Write  $\sum_j \Delta Q_{INJ} + \sum_{jk} \Delta Q_{LOSS} = 0$ 
8:   end if
9:    $j++$ 
10: end while

```

After constructing all the constraint equations, the next work is to identify which state variable will be changed, which is presented in the Algorithm 3. The number of changeable state variables within an area of attack depends on the type of node, such as slack bus, PV bus, or bad bus,

within it. Therefore, if the area of attack with n nodes contains a slack bus, which always has fixed value for both the voltage magnitude and voltage angle, it is apparent that the set of changeable state variables will be $(2 \times n - 2)$. Likewise, for the existence of a PV bus in an area of attack with n nodes, the set of changeable state variables will be $(2 \times n - 1)$. Since the set of constraint equations is nonlinear, an iterative numerical technique and approximate solutions are expected. For that reason, the relationship between the number of equations and the number of unknown or changeable state variables is important. For the sake of simplicity in this work, we aim at a designing process with the number of constraint equations being equal to the number of unknowns. Thus, if the number of changeable state variables in the area of attack is greater than the number of constraint equations, not every value of state variable will be manipulated during the attack design process.

Algorithm 3 Identifying changeable state variables

Input: Area of Attack Ω_A

Output: The set of changeable state variable SV

```

1: No. of SV  $n \leftarrow 2 \times \text{Sizeof}(\Omega_A)$ 
2:  $SV = \{ |V_j, \theta_j | j \in \Omega_A \}$ 
3: while  $j \in \Omega_A$  do
4:   if (type of node  $j$ ) = Slack then
5:      $n = n - 2$ 
6:     Remove  $|V_j$  and  $\theta_j$ 
7:   else if (type of node  $j$ ) = PV then
8:      $n = n - 1$ 
9:     Remove  $|V_j$ 
10:  else
11:     $j++$ 
12:  end if
13: end while
```

As soon as the solution for the set of the constraint equations is obtained, all the malicious measurement values are ready to be computed using the traditional bad flow formulas. Then, the complete set of measurements, or in other words the input data for the SE package, is formed by combining the set of valid measurements with the set of malicious measurements. The whole design process is illustrated with a case study of the WSCC's 9-bus system³⁰ in the next section.

3.2 | Case study –The WSCC's 9-bus Power System

The WSCC's 9-bus power system³⁰ in Fig. 2 is selected as the case study due to several reasons. With nine branches, three sources and three loads, it is large enough to represent a typical interconnected power system. More importantly, its datasheet provides us with adequate information about all generators. Some well-known IEEE benchmarking system such as IEEE 14-bus, IEEE 30-bus, IEEE 57-bus, etc., are all lacking of such data. In the current SE-oriented work, 48 measurements, with 24 active power measurements and 24 reactive power measurements, will be deployed. Among 24 measurements of each type, 18 are deployed to monitor power flows at each end of branches and 6 are used to acquire data of power injections at nodes.

The design scheme presented in the previous section is first applied here to illustrate the algorithm in finding the attack area. The extended Y_{bus} for this nine-bus system is given in Fig. 3. For instance, an FD attack is launched by choosing Bus 5 as the initial point. The detailed process is visually illustrated in Fig. 3, resulting in the area of attack including bus {5, 4, 7, 1, 6, 8, 2}. Assuming that this result is also the smallest possible area of attack, then we can move to the next phase of the design process.

For the nine-bus system, given the area of attack as identified above, the set of constraint equations will be formed as follows. Since there are two non-injection nodes within the area of attack, Bus 4 and Bus 7, the first constraint will render four equations in total, $\Sigma P_{4j} = 0$, $\Sigma Q_{4j} = 0$, $\Sigma P_{7j} = 0$, and $\Sigma Q_{7j} = 0$. In addition, the second constraint always renders two equations regardless of the configuration of the system, thus the set of constraints has six equations in total. The complexity of the two equations based on the second constraint depends upon the number of loads, sources and branches within the area of attack. In this case, there are six branches, including both transformer branches and lines, as well as three loads and two sources. In total, there are eleven terms in each equation from the second constraint. The detailed formation of each equation from the set of constraints is presented as below.

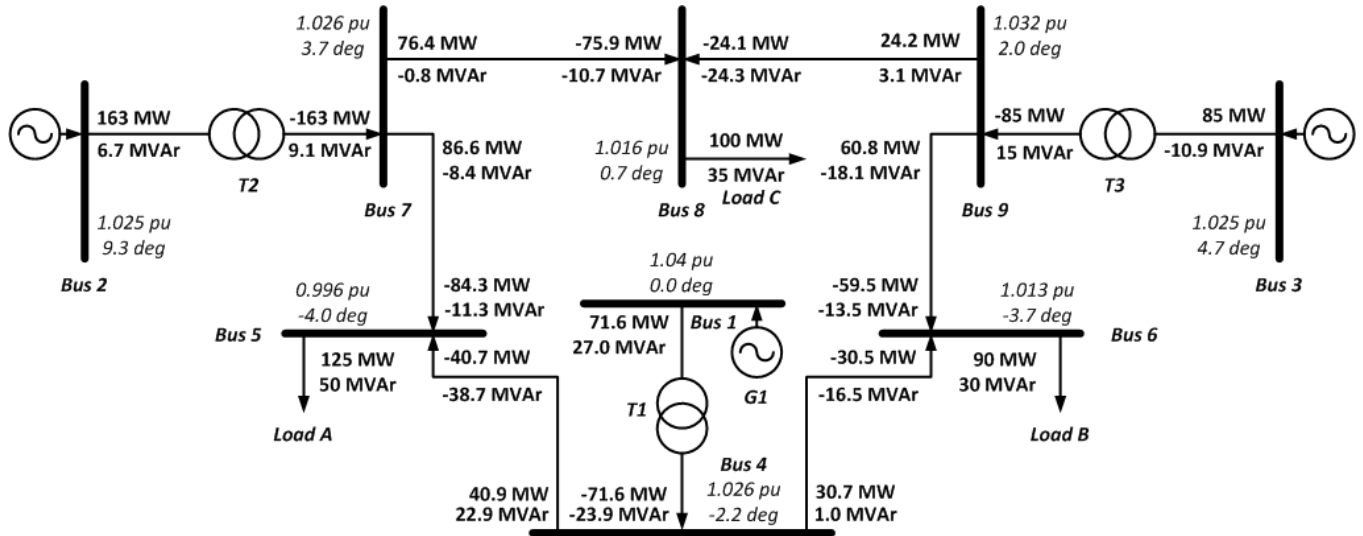


FIGURE 2 The nine-bus system and its load flow result.

Y_{11}	0	0	Y_{14}	0	0	0	0	0	0	-1
0	Y_{22}	0	0	0	0	Y_{27}	0	0	0	-1
0	0	Y_{33}	0	0	0	0	0	0	Y_{39}	-1
Y_{41}	0	0	Y_{44}	Y_{45}	Y_{46}	0	0	0	0	0
0	0	0	Y_{54}	Y_{55}	0	Y_{57}	0	0	0	1
0	0	0	Y_{64}	0	Y_{66}	0	0	0	Y_{69}	1
0	Y_{72}	0	0	Y_{75}	0	Y_{77}	Y_{78}	0	0	0
0	0	0	0	0	0	Y_{87}	Y_{88}	Y_{89}	0	1
0	0	Y_{93}	0	0	Y_{96}	0	Y_{98}	Y_{99}	0	0

○ Central node - - - > Scanning column
○ Subcentral node - > Checking node type
- > Returning to subcentral node

FIGURE 3 The extended Y_{bus} matrix for the nine-bus system and the process of identifying area of attack with central node is Bus 5.

1) The first constraint for the sum of active power and reactive power at no-injection Bus 4 and Bus 7

$$P_{41} + P_{45} + P_{46} = 0 \tag{1}$$

$$Q_{41} + Q_{45} + Q_{46} = 0 \tag{2}$$

$$P_{72} + P_{75} + P_{78} = 0 \tag{3}$$

$$Q_{72} + Q_{75} + Q_{78} = 0 \tag{4}$$

- 2) Parts of the second constraint for the sum of all changes in active and reactive power injections within the attack area (Equation (5) and Equation (6)) and for the sum of all changes in active and reactive power losses of all branches within the attack area (Equation (7) and Equation (8))

$$\Sigma \Delta P_{INJ} = \sum_{i=1,2,5,6,8} (P_i^{new} - P_i^{old}) \quad (5)$$

$$\Sigma \Delta Q_{INJ} = \sum_{i=1,2,5,6,8} (Q_i^{new} - Q_i^{old}) \quad (6)$$

$$\Sigma \Delta P_{LOSS} = \sum_{ij=14,27,45,46,57,78} (P_{L,new}^{ij} - P_{L,old}^{ij}) \quad (7)$$

$$\Sigma \Delta Q_{LOSS} = \sum_{ij=14,27,45,46,57,78} (Q_{L,new}^{ij} - Q_{L,old}^{ij}) \quad (8)$$

In the current example of the nine-bus system, the area of attack with six equations has already been identified. Among all nodes within the area of attack $\{1, 2, 4, 5, 6, 7, 8\}$, nodes 6 and 8 are the nodes with power injection at the boundary. In order to limit the affected range to reach no further than the boundary, we want to keep their state variables unchanged (both the voltage magnitudes and the voltage angles). From the rest of the set $\{1, 2, 4, 5, 7\}$, node 1 is the slack bus and node 2 is a PV node. Consequently, there are seven adjustable state variables within the area of attack $\{\theta_2, \theta_4, \theta_5, \theta_7, V_4, V_5, V_7\}$. Meanwhile, the current principle of attack design is about first choosing one state variable as an initial point of attack then solving the set of constraint equations for manipulated state variables, which, in turn, will be used to calculate the malicious measurement values. Thus, the requirement for the number of changeable state variables is, in fact, one unit more than the number of the constraint equations. In the current example, Bus 5 is chosen as an initial point by arbitrarily adjusting its angle by an amount of 0.5 degree. The next task is to solve the set of six nonlinear equations $\{\text{Equation (1), Equation (2), Equation (3), Equation (4), (5) + (7) = 0, (6) + (8) = 0\}$ for the six unknowns $\{\theta_2, \theta_4, \theta_7, V_4, V_5, V_7\}$.

In order to evaluate the result of the above design scheme, SE package of PowerFactory is employed. This package is equipped with all critical features that an industry-standard State Estimation package requires, including but not limited to receiving input/measurement data from Remote Telemetry Units (RTUs), checking plausibility, solving an optimization problem to find estimated values of state variables, checking observability, marking redundant data as well as bad data, etc. For the purpose of testing our design theory, eight different cases of attack are prepared (corresponding to the change of Bus 5 voltage angle of $\pm 0.5, \pm 1, \pm 1.5, \pm 2$ degrees).

All the eight attack schemes successfully bypassed BDD of the SE module in the PowerFactory package without being detected even just one false measurement. For the case with an initial +0.5 degrees adjustment at Bus 5 voltage angle, 34 out of 48 measurements were intervened (marked by the cell with gray shade) in Fig. 4. Deviation of each manipulated measurement from its steady-state value is significant, however, it is still able to avoid being discovered, due to the extremely small difference between the fed-in data and the calculated values by the SE (just around the order of 10^{-5} percent). These small values of difference greatly contribute to convincing the package for the authenticity, thus easily bypassing the BDD, even if the changes of bads at Bus 5, 6 and 8 through each case are significant. Without an additional measurement for detecting bad measurements, neither the system operator nor the program is able to reveal the existence of manipulated data. Information about all eight cases of attack is summarized in Table 1.

	Pij_New (MW)	Pij_Old (MW)	Qij_New (MVar)	Qij_Old (MVar)
B4-6	33.47893259	30.69265634	0.249026218	0.547461261
B6-4	-33.28619209	-30.52789584	-15.64282316	-16.09137671
B4-5	33.53196629	40.9585565	22.86656222	22.61451707
B5-4	-33.32718521	-40.70274178	-39.13897828	-38.44247158
B6-9	-59.47209936	-59.47209905	-13.9085818	-13.90862011
B9-6	60.82255604	60.82255575	-17.72588189	-17.72592219
B5-7	-82.02405566	-84.29724949	-12.08205662	-11.55752151
B7-5	84.19410879	86.59234546	-8.331567484	-8.21157004
B7-8	83.45429488	76.41573908	-1.579743124	-1.185429188
B8-7	-82.8896037	-75.9413277	-9.198677067	-10.35698807
B8-9	-24.05865046	-24.0586504	-24.64314987	-24.64301092
B9-8	24.14723794	24.14723789	3.412330256	3.412473933
B4-1	-67.01089907	-71.65121285	-23.11558813	-23.16197832
B1-4	67.01089907	71.65121285	25.86317896	26.26333532
B7-2	-167.6484037	-163.0080845	9.911310755	9.397000424
B2-7	167.6484037	163.0080845	6.808859593	6.408750792
B9-3	-84.96979147	-84.96979349	14.31344839	14.31344916
B3-9	84.96979147	84.96979349	-10.24308685	-10.24308752

FIGURE 4 Comparison between the manipulated and the steady-state measurement values on branches.

TABLE 1 Results from eight different attack cases.

Case	$\pm\theta_5(^{\circ})$	Plausibility Check	Observability	Bad Data
1	+0.5	0/48	Yes	0/34
2	-0.5	0/48	Yes	0/34
3	+1.0	0/48	Yes	0/34
4	-1.0	0/48	Yes	0/34
5	+1.5	0/48	Yes	0/34
6	-1.5	0/48	Yes	0/34
7	+2.0	0/48	Yes	0/34
8	-2.0	0/48	Yes	0/34

4 | FD IDATA GENERATION PROCESSES

As demonstrated in the above experimental results, our attack design can completely bypass the existing sophisticated BDD of an SE package. From this basis, we move forward to build up the first cyber-physical AC-based FD I dataset in power system, particularly, the transmission system's dataset of state estimation (namely, TSE-D S). The object of this task is still the W ECC's nine-bus system³⁰. It is complicated enough to be representative, yet simple enough to build up the dataset. In addition, its loading profile is generated with the available demand data of Tasmania (an island state of Australia) that can be easily collected from Australian Energy Market Operator (AEMO)³¹. The TSE-D S consists of a set of normal data, which reflects the results achieved from inputting the SE with genuine measurement values, and a set of attack data, which has been collected by running the State Estimation with data containing corrupted values. The process of generating this TSE-D S is described below.

4.1 | Normal steady-state dataset

Similar to various sample systems, the nine-bus system under investigation has only one loading data, corresponding to one steady state of operation. For this reason, a realistic demand data will be used to render different states of operation for this system. Among the available demand data from AEMO, it is the system of Tasmania State that shares a lot of similarities with the nine-bus system. Therefore, the historic demand data for Tasmania in 2018 is employed to construct various loading scenarios for the W ECC nine-bus system through a process of scaling down.

After collecting enough data about load demands for the system where 52558 values of demand were created, the next task was generating genuine measurement values, which in turn will become the input data for the SE process. Although this work seems to be simple with the load flow calculation of PowerFactory, it turns out to be extremely tedious due to the large volume of input data. The scripting feature of PowerFactory, DPL (D I G SILENT Programming Language³²) is used to automate the whole process. Corresponding to 52558 sets of load demands, there are 52558 sets of load flow results, thus the SE produced 52558 spreadsheets of SE result. For the sake of management, sheets are grouped into files with 432 sheets per file, which are equivalent to the data monitored in three consecutive days. Each spreadsheet contains the comprehensive SE results of 48 measurements in the nine-bus system. The order of measurements and the detailed information about each attribute in a spreadsheet can be found in Readme.txt file of the dataset. For every measurement, nine relevant attributes were recorded where the most important fields are the calculated measurement values and the BDD indication. In conclusion, there are 122 files containing different load demands, load flow results and state estimation results in the normal dataset. From the point of view of the intrusion detection researchers, the label for each measurement in this set is "normal".

4.2 | False Data Injection Attack dataset

The procedure of generating attack data is partly similar to the normal data generation except it employed load flow results as ingredient to produce the attack vectors (the corrupted measurements) before injecting into the SE. The stage of attack design is described in details in the previous section with the illustrated example using only one set of steady-state values to produce eight different sets of attack measurements. Although the number of attack cases can be generated as many as we want, for every steady state corresponding to a set of load demands, two scenarios of attack are enough to create a huge volume yet complicated attack data. This dataset has similar format to the normal dataset, which contains all relevant information about every measurement in the system as well as the results from the SE. However, the SE outputs do not include explicitly any information about the attack since the proposed attack design process is able to completely bypass the BDD of the PowerFactory. There are cases that the whole set of 48 measurements were manipulated while there are cases that only part of the set were attacked. However, it can be

confirmed that every spreadsheet in the folder "Attack_TAS" contains data about attack on the SE. In conclusion, the amount of attack records is twice as much as the amount of normal data. A brief summary of the TSE-DS dataset is shown in Table 2.

TABLE 2 Summary of the TSE-DS dataset.

Description	Values
Number of records/spreadsheets	157674
Number of normal records	52558
Number of attack records	105116
Number of attributes	9
Number of measurements per sheet	48
Number of active power measurements per sheet	24
Number of reactive power measurements per sheet	24
Number of Bad Data in normal records	0
Number of Bad Data in attack records	34-48
Number of Bad Data detected in attack records	0

5 | PRELIMINARY ANALYSIS OF THE GENERATED DATA SET

In this part, some preliminary analyses are carried on to examine the similarity between the normal data and attack data. Since the process of State Estimation involves both physical laws of electrical system as well as the stochastic optimization, the samples of dataset (one random record in each file of normal data and its corresponding record from the attack data) are inspected under both perspectives. The inspection results demonstrate causes for the failure of the BDD in revealing injected bad measurements.

5.1 | Electrical perspective

As stated above, the FD I attack fundamentally sets up a counterfeit steady state of operation based on collected data from a genuine state. Therefore, the deceitful state must satisfy all the physical constraints of a steady state in power system. Firstly, the power balance must be guaranteed. It means that the total amount of active and reactive power consumed by loads plus the sum of all power losses on branches must be equal to the generated active and reactive power, respectively. In addition, status of the nodes with no power injected must be maintained. For example, an assessment based on physical system criteria for Sheet 285th of file Norm all 22nd and its corresponding attack data is conducted. From the assessment results of the no-injection bus, the absolute maximum error for the sum of active power is around the order of 10^{-8} while the error for reactive power is even significantly smaller, around the order of 10^{-13} . It means that the largest error is as large as 0.01W for such calculation. In addition, the observed results implied no difference between attack data and normal data. The second assessment results related to the mismatch between consuming and generating is just around the order of 10^{-7} , which is only equivalent to 0.1W. Once again, the difference between normal and attack state is small enough and this looks the likely reason for the success in bypassing the BDD.

5.2 | Statistical analysis perspective

The problem of estimating state variables is solved continuously while the bad data, if exists, will be gradually excluded from the set of input data. This process is repeated until the set of input data contains only *suitable data*, not just *correct data*. This is a loophole that attackers can exploit to design manipulated measurements to bypass the BDD in the SE package. More specifically, as long as the manipulated values are systematically designed to be as close as possible to the appropriate values from the point of view of the package, the BDD will consider it as the normal data. The key of this issue originates from the mechanism of the BDD.

When it comes to the measurement values, it is apparent that they contain errors due to various reasons: configuration of transducers, wiring or transmitting issues, etc. It is impossible to acquire the exact values of both measurement and the corresponding errors. However, we usually assume

that the acquired values are close to the true value with only a small difference of error ϵ as below³³:

$$Z_{meas} = Z_{true} + \epsilon \quad (9)$$

The values of ϵ are unknown but assumed to have a normal probability density function with zero mean. Therefore, the residual $J(x)$ in Equation (10) must have the probability density function as chi-square distribution³⁴, $\chi^2(K)$ with K is the degree of freedom, calculated by Equation (11).

$$J(x) = \sum_{i=1}^{N_m} \frac{[Z_{meas} - Z_{calc}]^2}{\sigma_i^2} \quad (10)$$

$$K = N_m - N_s \quad (11)$$

where

- σ_i : Standard deviation of measurement i^{th} .
- N_m : Number of measurements in the system.
- N_s : Number of states, equal to $(2n - 1)$ with n is the number of nodes in the system.

The mechanism of BDD is simply by comparing the value of residual $J(x)$ with the value of the chi-square distribution for certain value of K at a significance level. The chosen value of significance level implies the false alarm occurrence created by the process of hypothesis testing³⁴. Likewise, a significance value of 0.005 means only 0.5 percent cases raise a false alarm. DgSILENT does not reveal the exact value of significance level in their SE package. Thus, in order to reduce the false alarm rate in a large data volume environment, in companion with the parameters of four current work $N_m = 48$ and $N_s = 17$, a significance level of 0.005 was chosen, resulting in the threshold to identify bad data being 53.67. It means that whichever set of input data that can bring out the residual of greater than 53.67 will be suspected to contain bad data and vice versa. The computation of $J(x)$ for generated data was conducted on the same samples from the electrical perspective. For instance, with data from Sheet 285th of file Norm all122nd and its corresponding attack data, both $J(x)$ values for attack (≈ 0.00224) and normal data ($\approx 2.21 \times 10^{-8}$) are small enough to avoid being marked as suspected, which is far below the threshold of 53.67. The same calculation procedure is conducted for one random record in each files of normal data and its corresponding record from the attack data, yielding the value of residual fluctuated around the order of 10^{-3} to 10^{-8} . These small values making the set of attack data having the full reputation as being the normal data. Therefore, the failure of the BDD is inevitable due to the similarities in both physical and statistical aspects of two types of dataset.

6 | CONCLUSION AND FUTURE WORK

In this paper, an AC model-based FD attack design scheme is proposed. A case study with industrial standard AC-based SE is used to demonstrate the scheme. The BDD, which is specifically equipped for the purpose of detecting and eliminating any inappropriate data, completely failed to notice the existence of manipulated measurements in the set of input data, even when they make up a majority of the data. This work distinguished itself from various works about DC-based SE, which is only a simplified linearized version of the AC counterpart. Several works in Section 2 also brought out the poor performance of DC-based SE systems. We have shown that the DC-based FD attack model where most of existing works are based on is unlikely successful in passing the AC-based commercial-scale BDD mechanism.

Traditionally, State Estimation is deployed for the transmission system only. However, as the integration of Distributed Energy Resources quickly spreads out in recent years, the implementation of SE in the distribution system is indispensable. The newly emerged distribution system will then have a much more sophisticated structure with bidirectional power flows. Subsequently, the system monitoring work will be more complicated than in the classical distribution system with radial feeder only. Thus, the security considerations in distribution systems are indispensable for future work. Since the structure of distribution system is getting closer and closer to the transmission system (meshed, various loads and sources, etc.), there exists an expectation that our proposed attack design is applicable to active distribution as well as undetectable with the existing commercial BDD mechanisms. Therefore, our cyber-physical dataset will be a valuable resource for the purpose of conducting research on system's defense strategies. The FD dataset TSE-D S can be acquired by sending email to the corresponding author Prof. Jiankun Hu at JH u@ adfa.edu.au.

ACKNOWLEDGEMENTS

This research is supported by ARC Discovery Grant (ID DP190103660)561 and ARC Linkage Grant (ID LP180100663).

References

1. Liu Y, Ning P, Reiter M K. False data injection attacks against state estimation in electric power grids. *ACM Transactions on Information and System Security (TISSEC)* 2011; 14 (1):13.
2. Hug G, Giam Papa JA. Vulnerability assessment of AC state estimation with respect to false data injection cyber-attacks. *IEEE Transactions on smart grid* 2012; 3 (3):1362-1370.
3. Bobba RB, Rogers KM, Wang Q, Khurana H, Nahrstedt K, Overbye TJ. Detecting false data injection attacks on dc state estimation. In: .2010.; 2010.
4. Anwar A, Mahmood AN, Pickering M. Modeling and performance evaluation of stealthy false data injection attacks on smart grid in the presence of corrupted measurements. *Journal of Computer and System Sciences* 2017; 83 (1):58-72. doi:<https://doi.org/10.1016/j.jcss.2016.04.005>
5. Digsilent's PowerFactory 2017 SP4. <https://www.digsilent.de/en/new-sreader/digsilent-releases-powerfactory-2017-sp4.html>;
6. KDD Cup 1999 Data. <http://kdd.ics.uciedu/databases/kddcup99/kddcup99.html>;
7. DARPA Intrusion Detection Data Sets. <https://www.llnwd.com/industry/defense/darpa-intrusion-detection-data-sets>;
8. Creech G, Hu J. A semantic approach to host-based intrusion detection system using contiguous and discontinuous system call patterns. *IEEE Transactions on Computers* 2013; 63:807-819.
9. Creech G, Hu J. Generation of a new IDS test dataset: Time to retire the KDD collection. In: ; 2013:4487-4492.
10. Next Generation Intrusion Detection System (NGIDS-DS): Overview. https://research.unsw.edu.au/sites/all/files/facultyadmin/ngids-ds_overview.pdf.
11. Liang G, Zhao J, Luo F, Weller SR, Dong ZY. A review of false data injection attacks against modern power systems. *IEEE Transactions on Smart Grid* 2017; 8 (4):1630-1638.
12. Yang Q, Yang J, Yu W, An D, Zhang N, Zhao W. On false data-injection attacks against power system state estimation: Modeling and countermeasures. *IEEE Transactions on Parallel and Distributed Systems* 2014; 25 (3):717-729.
13. Rahman M A, Mohsenian-Rad H. False data injection attacks with incomplete information against smart power grids. In: ; 2012:3153-3158.
14. Yu ZH, Chin WL. Blind false data injection attack using PCA approximation method in smart grid. *IEEE Transactions on Smart Grid* 2015; 6 (3):1219-1226.
15. Esmaifalak M, Nguyen H, Zheng R, Han Z. Stealth false data injection using independent component analysis in smart grid. In: ; 2011:244-248.
16. Liu X, Bao Z, Lu D, Li Z. Modeling of local false data injection attacks with reduced network information. *IEEE Transactions on Smart Grid* 2015; 6 (4):1686-1696.
17. Kin J, Tong L, Thomas RJ. Data framing attack on state estimation with unknown network parameters. In: ; 2013:1388-1392.
18. Kosut O, Jia L, Thomas RJ, Tong L. Limiting false data attacks on power system state estimation. In: ; 2010:1-6.
19. Liu L, Esmaifalak M, Ding Q, Emesh VA, Han Z. Detecting false data injection attacks on power grid by sparse optimization. *IEEE Transactions on Smart Grid* 2014; 5 (2):612-621.
20. Li S, Yin az Y, Wang X. Quickest detection of false data injection attack in wide-area smart grids. *IEEE Transactions on Smart Grid* 2015; 6 (6):2725-2735.
21. Huang Y, Li H, Campbell KA, Han Z. Defending false data injection attack on smart grid network using adaptive CUSUM test. In: ; 2011:1-6.
22. Bis, Zhang YJ. Graphical methods for defense against false-data injection attacks on power system state estimation. *IEEE Transactions on Smart Grid* 2014; 5 (3):1216-1227.
23. Xie L, Mo Y, Sinopoli B. False data injection attacks in electricity markets. In: ; 2010:226-231.

24. Anwar A, Mahmood AN. Vulnerabilities of smart grid state estimation against false data injection attack. In: Springer. 2014 (pp. 411–428).
25. Manandhar K, Cao X, Hu F, Liu Y. Detection of faults and attacks including false data injection attack in smart grid using Kalman filter. *IEEE transactions on control of network systems* 2014; 1 (4):370–379.
26. Chaojun G, Jintitijaroen P, Motani M. Detecting false data injection attacks in ac state estimation. *IEEE Transactions on Smart Grid* 2015; 6 (5): 2476–2483.
27. Liang J, Sankar L, Kosut O. Vulnerability analysis and consequences of false data injection attack on power system state estimation. *IEEE Transactions on Power Systems* 2016; 31 (5):3864–3872.
28. Rahmani MA, Mohsenian-Rad H. False data injection attacks against nonlinear state estimation in smart power grids. In: ; 2013:1–5.
29. Conservation of Energy. https://en.wikipedia.org/wiki/Conservation_of_energy;
30. Anderson PM, Fouad AA. *Power system control and stability*. John Wiley & Sons. 2008.
31. Australian Energy Market Operator's Data Dashboard. <https://www.aemo.com.au/Electricity/National-Electricity-Market-NEM/Data-dashboard>;
32. PowerFactory 2017 User's Manual. <https://www.digsilent.de/en/downloadshtml>;
33. Monticelli A. *State estimation in electric power systems: a generalized approach*. Springer Science & Business Media. 2012.
34. Wood AJ, Wollenberg BF, others. *Power generation, operation, and control*. John Wiley & Sons. 2013.

